Pharmacological Research 187 (2023) 106628

Contents lists available at ScienceDirect

Pharmacological Research

journal homepage: www.elsevier.com/locate/yphrs

Combination of palbociclib with navitoclax based-therapies enhances *in vivo* antitumoral activity in triple-negative breast cancer

Alejandra Estepa-Fernández [a,b,c], Alba García-Fernández [a,b,c,*], Araceli Lérida-Viso [a,b,c,d], Juan F. Blandez [a,c,d], Irene Galiana [a,b], Félix Sancenon-Galarza [a,b,c,d], Mar Orzáez [b,e,**], Ramón Martínez-Máñez [a,b,c,d,*]

[a] *Instituto Interuniversitario de Investigación de Reconocimiento Molecular y Desarrollo Tecnológico (IDM) Universitat Politècnica de València, Universitat de València. Camino de Vera, s/n, 46022 Valencia, Spain*
[b] *Unidad Mixta UPV-CIPF de Investigación en Mecanismos de Enfermedades y Nanomedicina, Universitat Politècnica de València, Centro de Investigación Príncipe Felipe. C/ Eduardo Primo Yúfera 3, 46012 Valencia, Spain*
[c] *CIBER de Bioingeniería, Biomateriales y Nanomedicina, Instituto de Salud Carlos III, Spain*
[d] *Unidad Mixta de Investigación en Nanomedicina y Sensores. Universitat Politècnica de València, IIS La Fe. Av. Fernando Abril Martorell, 106 Torre A 7ª planta, 46026 Valencia, Spain*
[e] *Centro de Investigación Príncipe Felipe, C/ Eduardo Primo Yúfera 3, 46012 Valencia, Spain*

ARTICLE INFO

Keywords:
TNBC
Senescence
Palbociclib
Senolytic
Navitoclax
Pro-drug

ABSTRACT

Triple-negative breast cancer (TNBC) is a very aggressive subtype of breast cancer with a poor prognosis and limited effective therapeutic options. Induction of senescence, arrest of cell proliferation, has been explored as an effective method to limit tumor progression in metastatic breast cancer. However, relapses occur in some patients, possibly as a result of the accumulation of senescent tumor cells in the body after treatment, which promote metastasis. In this study, we explored the combination of senescence induction and the subsequent removal of senescent cells (senolysis) as an alternative approach to improve outcomes in TNBC patients. We demonstrate that a combination treatment, using the senescence-inducer palbociclib and the senolytic agent navitoclax, delays tumor growth and reduces metastases in a mouse xenograft model of aggressive human TNBC (hTNBC). Furthermore, considering the off-target effects and toxicity derived from the use of navitoclax, we propose a strategy aimed at minimizing the associated side effects. We use a galacto-conjugated navitoclax (nav-Gal) as a senolytic prodrug that can preferentially be activated by β-galactosidase overexpressed in senescent cells. Concomitant treatment with palbociclib and nav-Gal *in vivo* results in the eradication of senescent hTNBC cells with consequent reduction of tumor growth, while reducing the cytotoxicity of navitoclax. Taken together, our results support the efficacy of combination therapy of senescence-induction with senolysis for hTNBC, as well as the development of a targeted approach as an effective and safer therapeutic opportunity.

1. Introduction

Breast cancer is one of the most common cancers in females and the leading cause of cancer-related death in women. Among all breast cancer subtypes, approximately 15–20% of them are triple-negative breast cancer (TNBC) [1,2]. TNBC is characterized by the lack of estrogen (ER) and progesterone receptor (PR) and human epidermal growth factor receptor 2 (HER2) amplification/overexpression [3]. It

Abbreviations: CDK, cyclin-dependent kinases; FDA, US Food and Drug Administration; HER2, human epidermal growth factor receptor 2; hTNBC, human triple-negative breast cancer; IC50, half maximal inhibitory concentration; nav-Gal, navitoclax prodrug; PI, Propidium iodide; PR, progesterone receptor; pRb, phosphorylated retinoblastoma protein; PROTAC, proteolysis-targeting chimera; Rb, retinoblastoma protein; SA-β-Gal, senescence-associated β-galactosidase; TIS, therapy-induced senescence; TNBC, triple-negative breast cancer.

* Corresponding authors at: Instituto Interuniversitario de Investigación de Reconocimiento Molecular y Desarrollo Tecnológico (IDM) Universitat Politècnica de València, Universitat de València. Camino de Vera, s/n, 46022 Valencia, Spain.

** Corresponding author at: Unidad Mixta UPV-CIPF de Investigación en Mecanismos de Enfermedades y Nanomedicina, Universitat Politècnica de València, Centro de Investigación Príncipe Felipe. C/ Eduardo Primo Yúfera 3, 46012 Valencia, Spain.

E-mail addresses: algarfe@etsia.upv.es (A. García-Fernández), morzaez@cipf.es (M. Orzáez), rmaez@qim.upv.es (R. Martínez-Máñez).

https://doi.org/10.1016/j.phrs.2022.106628
Received 17 May 2022; Received in revised form 29 November 2022; Accepted 20 December 2022
Available online 21 December 2022

has worse prognosis than other breast cancer subtypes. The lack of hormone receptor expression and the aggressive proliferative behaviour have limited by now the availability of effective therapies, restricting in most cases the standard of care to chemotherapy [4,5]. Consequently, there is an urgent need for developing non-cytotoxic, targeted therapies to improve the poor prognosis of this aggressive subtype of breast cancer.

From another point of view, senescence is a tumor-suppressing mechanism that has been explored as a therapy for several tumors [6–9]. This therapy is already a reality in the clinical practice, for instance, by the use of cell cycle inhibiting drugs such as palbociclib, a highly selective inhibitor of cyclin-dependent kinases 4 and 6 (CDK 4/6). Palbociclib induces cellular senescence in the tumor, thus limiting tumor progression, and has been approved by the US Food and Drug Administration (FDA) to treat first-line endocrine-based therapy for postmenopausal women with hormone receptor-positive (HR+)/human epidermal growth factor receptor 2 negative (HER2 −) advanced or metastatic breast cancer in combination with letrozole or fulvestrant [10–12]. The good results obtained with this drug has encouraged the study of palbociclib treatment in TNBC patients (NCT03756090, NCT04360941, NCT04494958) [13]. However, despite the benefits of growth suppression after senescence induction in tumors, it has also been demonstrated that the accumulation of senescent cells promotes inflammation, angiogenesis, and can cause cancer recurrence by facilitating senescence escape or invasiveness [6,9,14,15].

In this scenario, the use of senolytics, drugs that specifically kill senescent cells, has been proven to be an effective remedy for alleviating such unwanted senescent cell accumulation [9]. Among senolytic drugs, navitoclax has been validated in a variety of preclinical models showing high potency in killing senescent cells, reducing cancer relapses and delaying ageing-related diseases [14,16–18]. Navitoclax inhibits the anti-apoptotic proteins Bcl-2, Bcl-xL and Bcl-w [19]. Senescent cells, in many cases, depend on Bcl-xL for their survival [20], but other cells in the body, such as platelets, do as well [21]. Therefore, inhibition of Bcl-xL causes thrombocytopenia, the major dose-limiting toxicity effect which has restricted navitoclax use in the clinic [17,22]. In this context, it has been recently demonstrated that navitoclax harmful effects can be reduced by the design of pro-drugs [23] and nanodevices that selectively deliver navitoclax in senescent cells [6,8,9]. Galacto-conjugation of navitoclax with acetylated galactose results in the senolytic prodrug called nav-Gal that can preferentially be activated by β-galactosidase overexpressed in senescent cells. Previous studies from our group based on a similar strategy results in the selective detection of senescent cells [24,25]. The nav-Gal prodrug has been effective in reducing tumor size in orthotopically transplanted murine lung adenocarcinoma cells and in a tumor xenograft model of human non-small-cell lung cancer by combining senescence-inducing chemotherapies with the senolytic treatment, where it shows reduced hematological toxicity [23].

Based on the above, in this work, we explore the combination of senescence induction and the subsequent elimination of senescent cells (senolysis) as an alternative approach to improve outcomes in TNBC patients. Here, we demonstrate that palbociclib therapy-induced senescence (TIS) followed by adjuvant therapy with navitoclax causes a synergistic elimination of senescent cells, reduction of tumor growth and lung metastasis while decreasing the cytotoxicity of navitoclax in a xenograft mice model of aggressive human TNBC (hTNBC). Our findings support that senescence-inducing therapies combined with senolysis can be a promising strategy for the effective treatment of hTNBC. Moreover, targeted navitoclax-based therapies could facilitate its clinical use as an effective and safer strategy.

2. Results

2.1. Palbociclib induces senescence in MDA-MB-231

Firstly, we studied the capability of palbociclib to induce senescence in hTNBC. For that purpose, MDA-MB-231 cells were treated with palbociclib 5 μM for 7 days, and the senescence-associated β-galactosidase (SA-β-Gal) activity was evaluated. We observed increased positivity for SA-β-Gal staining in cells treated with palbociclib (Fig. 1 A). Inhibition of CDK4/6 signaling pathway by palbociclib treatment produces the hipophosphorylation of retinoblastoma protein (pRb), causing cell cycle arrest in the G1/S transition phase [26]. In palbociclib-treated MDA-MB-231 cells, a decrease in the phosphorylation of the pRb protein and an increase in the expression of p53 protein is observed when compared to non-treated cells (Figs. 1B, 1 C and S1), indicative of senescence induction. We also check the expression of CDK4 and CDK6 proteins after palbociclib treatment (Fig. S2), yet non-significant changes were observed.

To corroborate cell cycle arrest in palbociclib-treated cells, the expression of the Ki67 proliferation marker was analyzed by immunofluorescence (Fig. 1D). Control proliferating MDA-MB-231 cells shows a high expression of Ki67 (red emission), whereas palbociclib-treated cells lose the expression of the proliferation marker. Cell cycle analyses by flow cytometry demonstrated accumulation of cells in the G1-phase, thus corroborating the cell cycle arrest (Fig. 1E). Altogether these results confirm that palbociclib induces senescence in MDA-MB-231 hTNBC cells.

2.2. Navitoclax and nav-Gal are effective senolytics in TNBC

Once demonstrated the capability of palbociclib to induce senescence in hTNBC cells, we wondered if navitoclax or galacto-conjugated navitoclax, nav-Gal, could be effective for the selective elimination of senescent-hTNBC cells. Navitoclax is preferentially released from the nav-Gal prodrug due to the hydrolysis of the galactose unit in senescent cells (Fig. 2 A) as they have increased activity of senescence-associated β-galactosidase [23]. Navitoclax will trigger apoptosis by inhibiting Bcl-2, Bcl-w and Bcl-xL proteins causing Bax/Bak oligomerization in the mitochondria membrane [19]. Nav-gal synthesis was confirmed by HPLC-MS (Fig. S3).

In a first step, we demonstrated that palbociclib-treated hTNBC MDA-MB-231 cells overexpress the anti-apoptotic proteins Bcl-2, Bcl-xL and Mcl-1 (40 kDa) and downregulate the expression pro-apoptotic proteins such as Bax and Puma (Fig. 1 F, 1 G and S1). The Bcl-2-expression profile of senescent MDA-MB-231 cells indicates that the inhibition of Bcl-xL and Bcl-2 by navitoclax could be a potential strategy to eliminate senescent hTNBC cells [27]. In addition, treatment with specific Bcl antiapoptotic proteins inhibitors (ABT-199 for Bcl-2 inhibition, S63825 for Mcl-1 inhibition, and WeHi-539 for Bcl-xL inhibition) (Fig. S4), shows a slight reduction in cell viability in palbociclib-treated MDA-MB-231 after the specific inhibition of Bcl-xL by WeHi-539 and the specific inhibition of Mcl-1 by S63825 but not after the specific inhibition of Bcl-2 by ABT-199. When a more potent single agent Bcl-xL inhibitor, like A-1155463, was used, a similar effect to navitoclax was achieved for eliminating senescent hTNBC cells. Besides, its combination with the Bcl-2 inhibitor ABT-199 results in an additional cytotoxic effect. The results confirmed the potential of using inhibitors of anti-apoptotic proteins, such as navitoclax or A-1155463, to selectively kill senescent cells.

Then, to test the senolytic effect of both navitoclax and the prodrug nav-Gal against senescent cells, we performed cell viability studies in palbociclib-induced MDA-MB-231 senescent cells (treated with 5 μM palbociclib for 7 days) and proliferating cells treated with increasing concentrations of either navitoclax (Figs. 2B and 2 C) or nav-Gal (up to 10 μM) for 72 h (Figs. 2B and 2D). Navitoclax eliminates senescent MDA-MB-231 cells with an estimated half-maximal inhibitory concentration (IC50) value of 0.5 μM, whereas IC50 for nav-Gal is 0.7 μM (Fig. 2E). In addition, IC50 values of 1.3 μM and 2.7 μM were found for navitoclax and nav-Gal, respectively, in control cells. From these data, a senolytic index of 2.6x and 3.9x was found for navitoclax and nav-Gal. The senolytic index was calculated by measuring the ratio of the IC50

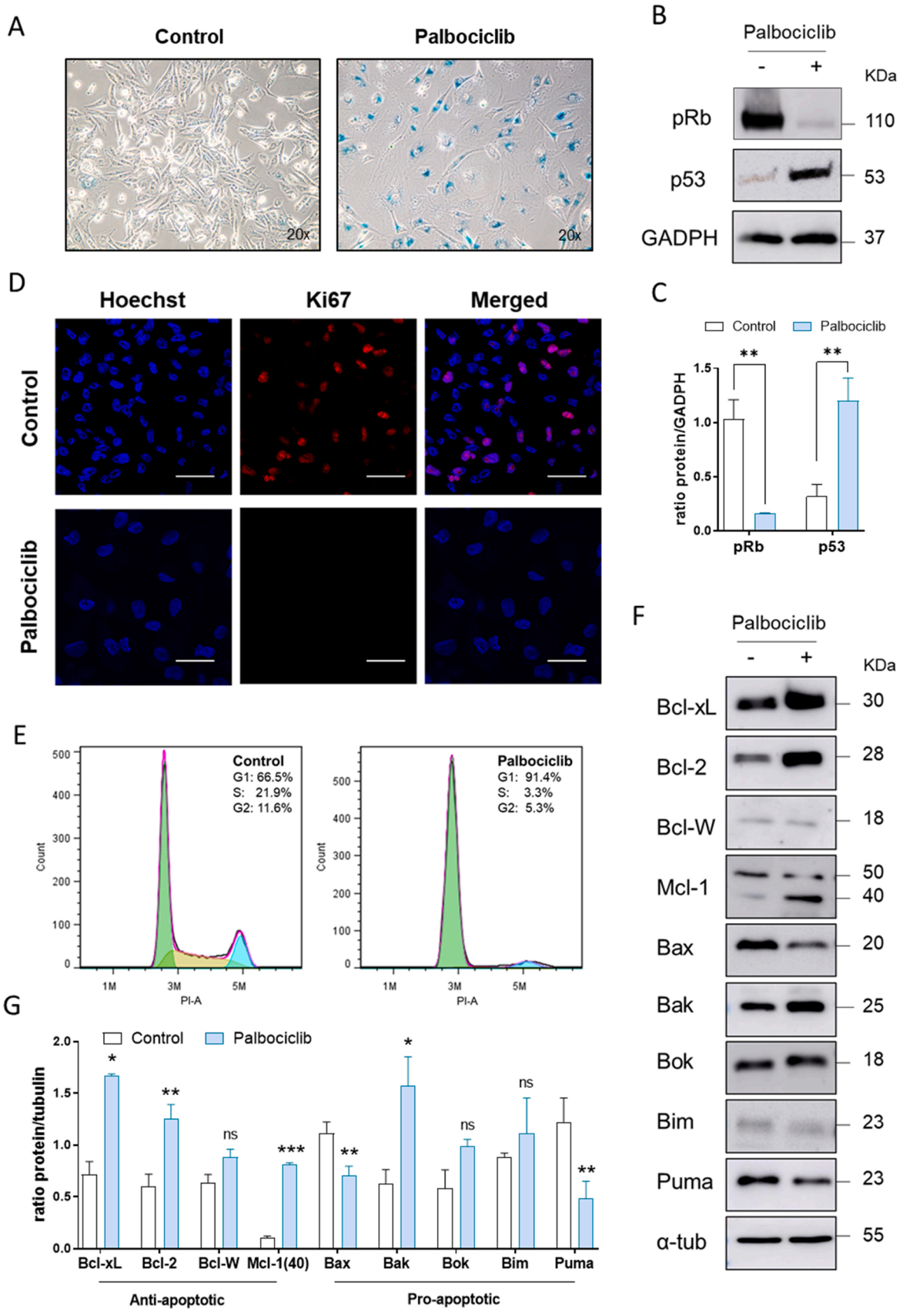

(caption on next page)

Fig. 1. Palbociclib induces senescence in MDA-MB-231. (A) β-Galactosidase staining (blue colour) of control (untreated proliferating cells) and 5 μm palbociclib-treated MDA-MB-231 cells. (B) pRb and p53 expression was evaluated in proliferating (-) and palbociclib-treated (+) MDA-MB-231 cells by western blot. (C) Quantification of western blot using Image J software. Data represent the mean ± SEM of at least three independent experiments and statistical significance was assessed by unpaired T-test (*$p < 0.05$; **$p < 0.01$). (D) Ki67 immunofluorescence images show staining of Ki67 (red) and nuclei stained with Hoechst (blue) in control cells. Scale bars, 20 μm. (E) Propidium iodide (PI) staining of proliferating and palbociclib treated MDA-MB-231 cells. Senescent cells accumulate in cell cycle G1-phase after 7 days of palbociclib treatment. (F) Western blot characterization of Bcl-2 family proteins in proliferating (-) and palbociclib-treated (+) MDA-MB-231 cells. (G) Quantification was performed using Image J software. Data represent the mean ± SEM of at least three independent experiments and statistical significance was assessed by unpaired T-test (*$p < 0.05$; **$p < 0.01$; ***$p < 0.001$).

values between control and senescent cells. Nav-Gal treatment improved specificity (higher senolytic index) compared to free navitoclax for hTNBC cells, mainly due to nav-Gal reduced toxicity in control cells compared to navitoclax. We also tested the senolytic activity of simultaneous co-treatment with palbociclib (5 μM) and navitoclax (1.25 μM) (Fig. S5) for 72 h. As expected, no effect was observed with simultaneous co-treatment. It is necessary to previously induce senescence in order to trigger senolysis with navitoclax. All these results confirmed the senolytic properties of navitoclax and nav-Gal in senescent hTNBC cells and indicate that nav-Gal has lower cytotoxic activity in non-senescent cells.

Additionally, we found that treatment with either navitoclax or nav-Gal (1 μM) induced apoptosis (assessed by increased Annexin V staining) preferentially in palbociclib-induced MDA-MB-231 senescent cells, in accordance with previously described results (Fig. 2 F) [23]. A strong signal for Annexin V (early and late apoptosis) was observed for both navitoclax (~40% of cells) and nav-Gal (~32% of cells) at equivalent doses after 48 h of treatment. The results demonstrate that both navitoclax and nav-Gal senolytics induce apoptosis in senescent cells.

2.3. Combinational treatment of palbociclib and navitoclax or palbociclib and nav-Gal reduce tumour volume in MDA-MB-231 xenografts

The *in vivo* effectivity of the dual treatment, i.e. palbociclib-inducing senescence therapy followed by either navitoclax or nav-Gal treatment (senolysis), was evaluated in MDA-MB-231 orthotopic hTNBC mouse model. To establish xenografts, MDA-MB-231 breast cancer cells were injected into the second lower right fat-pad of 6–7 weeks old nude BALB/C mice. When tumour volume reached an average of 60 mm^3, daily therapy was initiated with either vehicle (sodium lactate) or 50 mg/kg palbociclib (*via* oral gavage) (Fig. 3 A). To have an appropriate therapeutic window to study the combinational treatment, one day after starting palbociclib treatment, navitoclax administration was initiated either as a free drug (navitoclax, *via* oral gavage) or as a prodrug (nav-Gal, *via* i.p. injection) at the same molar dose.

As a result of palbociclib treatment, a significant decrease in tumour growth is observed (Figs. 3B and 3 C) due to the proper induction of senescence in the tumours, confirmed by an increased in X-gal staining (Fig. 3D). Treatment with navitoclax alone produces a slight non-significant reduction in tumour volume compared to control mice. In contrast, dual treatment with palbociclib and navitoclax or nav-Gal significantly reduced tumour growth. Concomitant treatment with either palbociclib and navitoclax or palbociclib and nav-Gal reduces animal weight (Fig. S6); however, no noteworthy toxicity was found after the treatment (Fig. S7).

Evaluation of lung metastases in MDA-MB-231 xenograft mice reveals the appearance of initial metastatic cell clusters in lung sections (Fig. 3E). Interestingly, after palbociclib treatment the number of metastatic nodes in the lung increases (Fig. 3E), while a significant decrease is detected in animals co-treated with palbociclib and navitoclax either as a drug or as prodrug (nav-Gal) (Fig. 3 F).

Furthermore, histological analyses of the tumors revealed that palbociclib treatment results in increased levels of p53 immunostaining (Fig. 4 A and 4B), which is a characteristic of cancerous cells in the senescent state. Concomitant treatment with palbociclib and navitoclax or nav-Gal reduced p53 expression, alongside a strong cell death induction, as illustrated by the increase in TUNEL signal (Fig. 4 A and 4 C). These results strongly suggest that apoptosis of senescent cells facilitates the antitumoral effect of co-treatments. Together these results confirm the benefits of the use of pro-senescent and senolytic therapy in hTNBC xenografts in reducing tumour growth and cancer dissemination to distant organs.

3. Discussion and conclusion

Triple-negative breast cancer (TNBC) is defined as the type of breast cancer that lacks estrogen, progesterone, and HER2 receptors [3]. Due to the loss of such receptors, TNBC is not sensitive to endocrine therapy or molecular targeted therapy. Therefore, treatment options for advanced TNBC patients are limited and ineffective [28,29], with a mortality rate of TNBC patients of 40% within the first 5 years after diagnosis [30]. Thus, therapeutic advancements are critical to improving mortality associated with TNBC.

The induction of senescence is a well-established tumour suppressive mechanism due to the characteristic proliferation arrest of senescent cells [31–35]. Different classical anticancer therapeutic strategies have been demonstrated to induce senescence in the tumor, such as chemotherapeutic agents, the use of radiotherapy or treatments with CDK4/6 inhibitors [36,37]. Chemotherapeutic drugs that are used widely clinically and have shown to induce senescence *in vivo* include doxorubicin [38], etoposide [39], cisplatin [40], bleomycin or temozolomide [41]. The clinically used CDK4/6 inhibitors, palbociclib, abemaciclib, and ribociclib also show senescence induction *in vivo* [42–45].

Despite the benefits of stopping cancer proliferation, it has been demonstrated that an excessive accumulation of senescent cells and their secretory phenotype can promote chronic inflammation, angiogenesis, or increase tumour promoting properties that may cause cancer recurrence [9,46–49]. Although senescence has always been considered as a permanent and irreversible cell cycle arrest, recent studies have suggested that, under certain conditions, therapy-induced senescent (TIS) tumor cells can escape from this condition and re-enter the cell cycle, thus acquiring an aggressive character [50–54].

On this basis, interventions aimed to limit the deleterious roles of senescent cells are under development *via* the design of senoblockers (drugs that inhibit senescence before it happens), senomorphics (drugs that inhibit senescence-associated secretory phenotype) and senolytics (drugs that eliminate senescent cells) [55]. Senolytics have been intensively investigated and are already being studied in clinical trials, with very positive preliminary results using dasatinib plus quercetin in patients with idiopathic pulmonary fibrosis and diabetic kidney disease [56,57]. Among senolytics, inhibitors of Bcl-2 anti-apoptotic proteins such as navitoclax have proved to be effective in reducing relapse in some cancer models and the onset of several aging associated-diseases [14,16–19]. Monotherapy with navitoclax has shown a good antitumoral activity in *in vivo* studies of small cell lung cancer, leukaemia, and lymphoma [58,59]. In the case of breast cancer, navitoclax is not sufficient to induce tumour death in some breast cancer cell lines [60], as we have also observed in MDA-MB-231 xenografts (*vide ante*). However, to enhance the efficacy of navitoclax, combined therapy with TIS agents, such as palbociclib or doxorubicin, has been recently proposed [6,7,61, 62]. Besides, several phase 1 and phase 1/2 clinical trials combining senescence-inducing chemotherapy and navitoclax are ongoing or completed, including the combination of navitoclax with cisplatin (NCT00878449), etoposide (NCT00878449) or osimertinib (NCT02520778) in lung cancer patients and with dabrafenib or

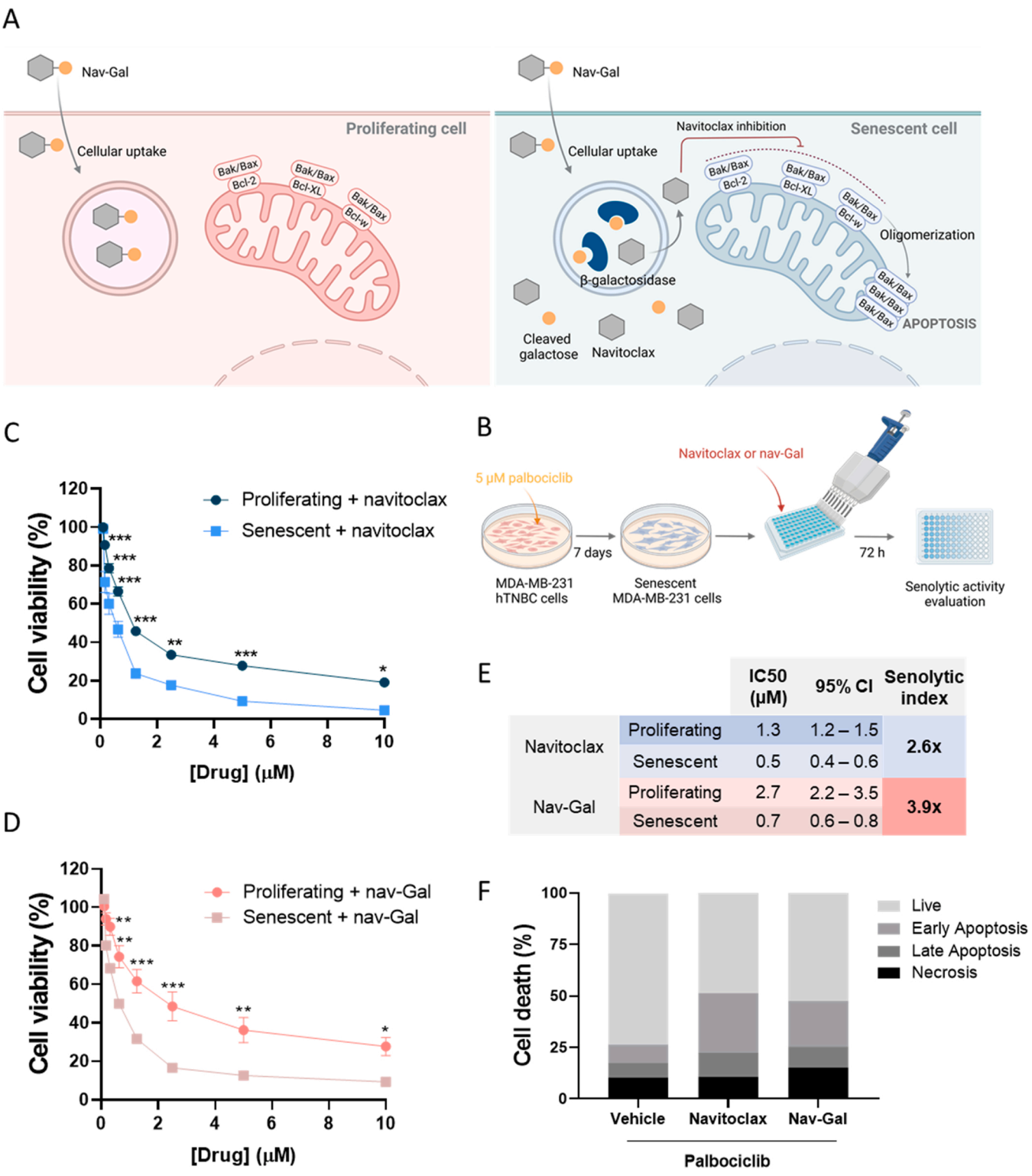

Fig. 2. Nav-Gal, a senolytic prodrug based on galacto-conjugation of navitoclax, is an efficient strategy for senolysis in TNBC MDA-MB-231 cells. (A) Scheme of the mechanism of action of the nav-Gal prodrug. Nav-Gal crosses the cell membrane through passive internalization. As senescent cells have increased activity in senescence-associated β-galactosidase, navitoclax is released by the hydrolysis of the galactose reaching its target proteins in the mitochondria (Bcl-2, Bcl-w and Bcl-xL). The inhibition of BCL-2 anti-apoptotic proteins by navitoclax causes Bax/Bak oligomerization in the mitochondria membrane triggering apoptosis. (B) Scheme of the sequential palbociclib plus navitoclax or nav-Gal treatments. Senescence in MDA-MB-231 cells were induced with 5 μM palbociclib treatment for 7 days. After 7 days, proliferating and senescent cells were plated and treated with navitoclax or nav-Gal. (C) Cell viability after 72 h of cell treatment with different concentrations of navitoclax (C) or nav-Gal (D) in proliferating and senescent MDA-MB-231 cells. All values are represented as a percentage of ($n \geq 3$) ± SEM, and statistical significance was assessed by two-way ANOVA followed by Sidak's post-tests (*$p < 0.05$, **$p < 0.01$, ***$p < 0.001$). (E) IC50 and senolytic index of navitoclax or nav-Gal treatment in proliferating and senescent MDA-MB-231 cells. (F) Cell death percentage (%) of early apoptotic, late apoptotic, and necrosis cells after vehicle (DMSO), navitoclax and nav-Gal (1 μM) treatments for 48 h. Percentages were measured by Annexin V-FITC and PI expression in flow cytometry. All values are represented as a percentage of ($n = 3$) ± SEM and statistical significance was assessed by two-way ANOVA followed by Sidak's post-tests (**$p < 0.01$, ***$p < 0.001$).

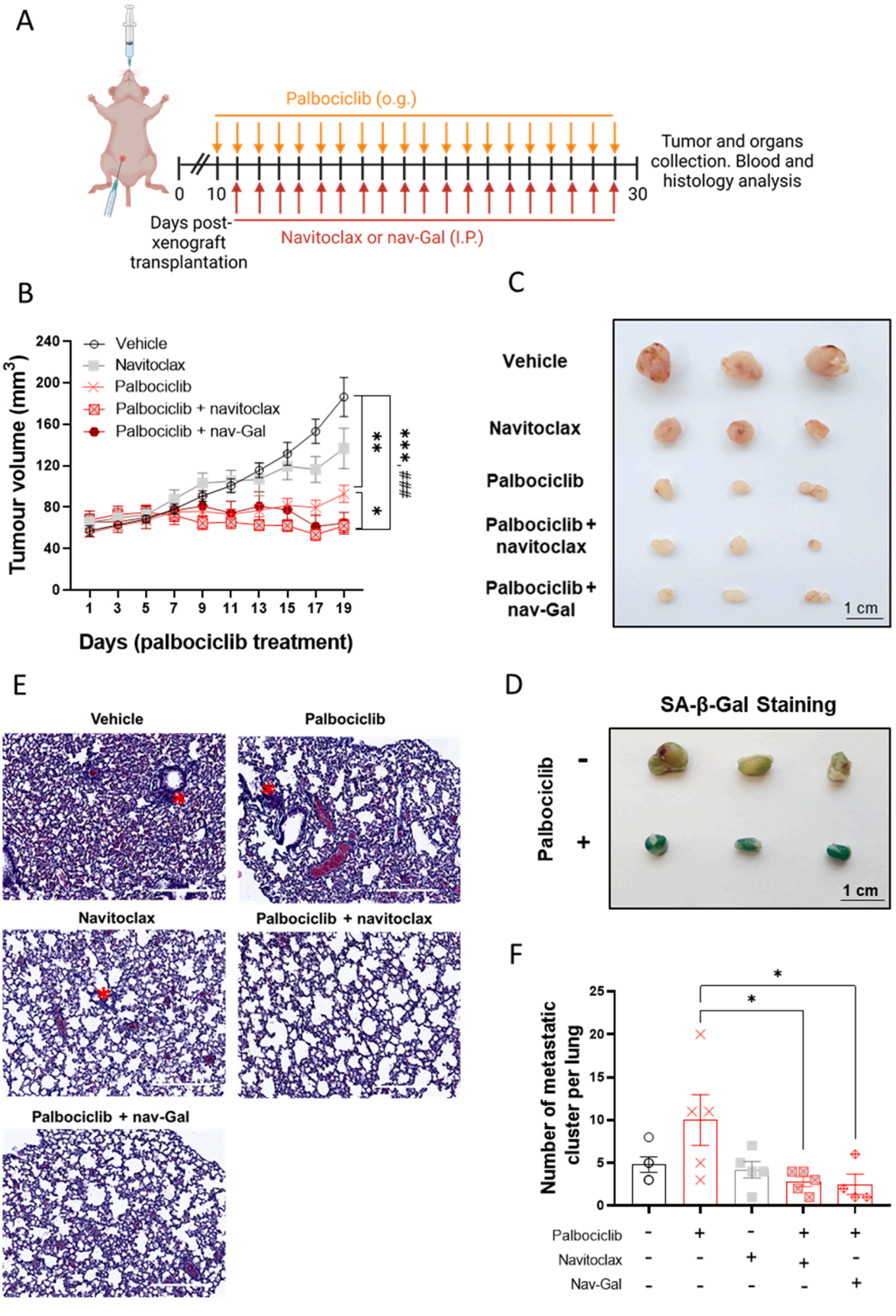

(caption on next page)

Fig. 3. Concomitant treatment of palbociclib and navitoclax-based therapies reduce tumor size and metastatic burden. (A) BALB/c nude female mice were orthotopically injected with MDA-MB-231 breast cancer cells and treated daily with either vehicle or palbociclib. 2×10^6 MDA-MB-231 cells were subcutaneously implanted on mammary pads. When tumours volume reached 60 mm^3, palbociclib treatment started and was maintained daily (o.g.) for 20 days. Navitoclax and nav-Gal daily treatments started one day after palbociclib treatment (navitoclax: o.g., navi-Gal: i.p., molar equivalents). Vehicle stands for the drug solvents: 50 mM sodium lactate pH 4.5 (o.g.) and 15% DMSO/ 85% PEG-400 (i.p.). (B) Tumour volume (mm^3) of the different treatment approaches during all the treatment. Statistical analysis was carried out using GraphPad Prism 8 and results were compared by one-way ANOVA followed by Tukey's post-tests (***Vehicle vs palbociclib + navitoclax; ###vehicle vs palbociclib + nav-Gal) (*$p < 0.05$; **$p < 0.01$; ***$p < 0.001$; ###$p < 0.001$). Data represent the mean ± SEM ($n = 5$). (C) Pictures of representative tumor samples for each treatment. Scale bar, 1 cm. (D) Pictures of representative tumor samples stained with X-gal. Scale bar, 1 cm. (E) H&E staining of representative lung sections taken from xenograft MDA-MB-231 tumour-bearing mice for metastatic clusters evaluation. Scale bar, 500 μm. (F) Quantification of metastatic lung clusters. Representative tissues images were microscopically counted. Statistical analysis was carried out using GraphPad Prism, and results were compared by one-way ANOVA followed by Tukey's post-tests (*$p < 0.05$). Data represent the mean ± SEM ($n = 5$).

trametinib for patients with metastatic melanoma (NCT01989585). Navitoclax has also been combined with gemcitabine (NCT00887757), paclitaxel (NCT00891605), docetaxel (NCT00888108), irinotecan (NCT01009073), erlotinib (NCT01009073), sorafenib (NCT02143401) or trametinib (NCT02079740) in advanced solid tumours [63].

Palbociclib induces senescence by inhibiting the activity of the cyclin D-CDK4/6 kinases complex by targeting the ATP-binding domains of CDKs 4 and 6 kinases which results in a decrease in the phosphorylation of Rb protein and subsequently induces G1 cell cycle arrest [64–68]. Furthermore, palbociclib has become the standard first-line therapy for advanced metastatic ER+ , HER2- negative breast cancer, used in combination with letrozole or fulvestrant [10,12,69,70]. Palbociclib in combination with letrozole significantly prolonged median progression-free survival (PFS) compared with placebo plus letrozole (27.6 vs 14.5 months) [71]. Although the effects of palbociclib in TNBC are not well-documented, cell cycle inhibition by palbociclib in MDA-MB-231 suggests its potential use to treat TNBC tumours [13, 72–74]. In addition, beneficial effects have already been found in TNBC by combining palbociclib plus other apoptotic drugs *in vitro* and *in vivo*. For instance, concomitant treatment of palbociclib plus enzalutamide enhanced the palbociclib-induced cytostatic effect in hTNBC MDA-MB-231 cells [72]. Besides, the combination of palbociclib plus cisplatin delayed tumour growth in MDA-MB-231 xenografts [13].

In this work, we demonstrate that palbociclib treatment induces senescence in xenograft mice bearing hTNBC MDA-MB-231. In addition, treatment with palbociclib followed by navitoclax-based therapies (navitoclax or nav-Gal) results in the reduction of tumour size and the number of metastatic lung clusters. This two-step pro-senescence/ senolytic combinatorial treatment regimen selectively induces apoptosis in hTNBC MDA-MB-231 senescent cancer cells causing synergistic reduced tumour growth. In addition, evaluation of lung metastases in the xenograft mice hTNBC model revealed the appearance of initial metastatic cell clusters in lung sections, while a significant decrease in the number of metastatic nodes in animals co-treated with palbociclib and navitoclax or nav-Gal were observed. Previous work from our group already demonstrated that palbociclib treatment in the 4T1 TNBC mouse model increases metastatic clusters in lungs as a consequence of the induction of senescence in the endothelium, and after subsequent senolysis with navitoclax the metastatic burden decreased [9]. This is relevant as metastasis has a significant role in the clinical management of TNBC. Currently, approximately 25% of TNBC patients relapse with distant metastasis [29]. The reduction of the tumour size and metastatic lung clusters found in this work provide strong support for the potential translation involving palbociclib treatments together with navitoclax in TNBC tumours.

As far as we know, this work is the first time that the combination of palbociclib-induced senescence followed by navitoclax-senolysis in hTNBC has been tested and shown to be effective [75]. In a previous work, we described the effective combination of palbociclib plus navitoclax in a 4T1 mouse model, which is usually considered a TNBC model [6]. Our work here translates the use of the combination of palbociclib plus navitoclax to a hTNBC model. When comparing both models, we have found that monotherapy with palbociclib has a more activity arresting the tumour in human MDA-MB-231 xenografts than in 4T1 orthotopic mice models, meaning that senolytic therapy have a better effect in human xenografts. These differences highlighting the importance of validating the combination of palbociclib plus navitoclax in both preclinical orthotopic mice and human xenographs models with the objective to make the potential transfer of the treatment to clinical practice more reliable.

Despite its efficacy in preclinical trials, the side effects of navitoclax have limited its translation to clinical practice. Among side effects of navitoclax, thrombocytopenia is the most relevant due to platelets dependence on Bcl-xL protein for their survival [76]. To overcome navitoclax toxicity, recently, a second generation of senolytics have been reported, such as the PZ15227, a Bcl-xL proteolysis-targeting chimera (PROTAC) of navitoclax with limited platelet toxicity [77]. Additionally, several prodrugs and nanodevices based on β-galactosidase overexpression in senescent cells have been reported [6,8,9,78,79], such as the prodrug nav-Gal [23], the galactose-modified duocarmycin [80], or the gemcitabine-derivative SSK1 [81]. In this scenario here, we proposed the use of the senolytic prodrug nav-Gal as a targeted strategy to reduce navitoclax toxicity. This galacto-conjugated navitoclax is preferentially activated in senescent cells by the elevated levels in senescent cells of SA-β-gal activity. Nav-Gal prodrug has proved to be effective after concomitant treatment with cisplatin in xenografts mice bearing of human A549 lung cancer cells and in orthotopic mice model using murine lung adenocarcinoma cells [23]. Our study demonstrated that a combination of palbociclib and nav-Gal treatment results in more selectively MDA-MB-231 senescent cells elimination over non-senescence cells. Besides, the concomitant treatment *in vivo* results in the effective elimination of senescent hTNBC cells with the subsequent reduction of tumor growth. Our previous results corroborated the proper reduction of platelet toxicity after galacto-conjugation compared navitoclax in *ex vivo* experiments with both human and murine blood samples [23]. Additionally, platelet count of wild-type C57BL/6 J treated daily with senotherapy for a total of 10 days exhibited severe thrombocytopenia after navitoclax treatment at day 5 [23]. This effect was also observed in the human lung cancer xenograft mice model treated with the combined cisplatin-induced senescence and navitoclax senolysis, whereas nav-Gal treatment did not cause this hematological toxicity [23].

Together our results demonstrate the combination efficacy of palbociclib plus navitoclax-based therapies, providing a strong support for a translational paradigm involving cell cycle arrest treatments together with anti-apoptotic inhibitors in TNBC tumors. Also, we have demonstrated that galacto-conjugation of navitoclax can be used as an effective approach to target senescent cells and limit the toxicity associated with free navitoclax. Overall, we show a safer and more effective therapeutic possibility for the treatment of hTNBC.

4. Experimental section

4.1. Cell culture and senescence induction

Human breast triple-negative adenocarcinoma MDA-MB-231 cells (ATCC) were cultured in DMEM (Sigma) supplemented with 10% fetal bovine serum (FBS; Sigma) and maintained at 37 °C in 5% CO_2. For

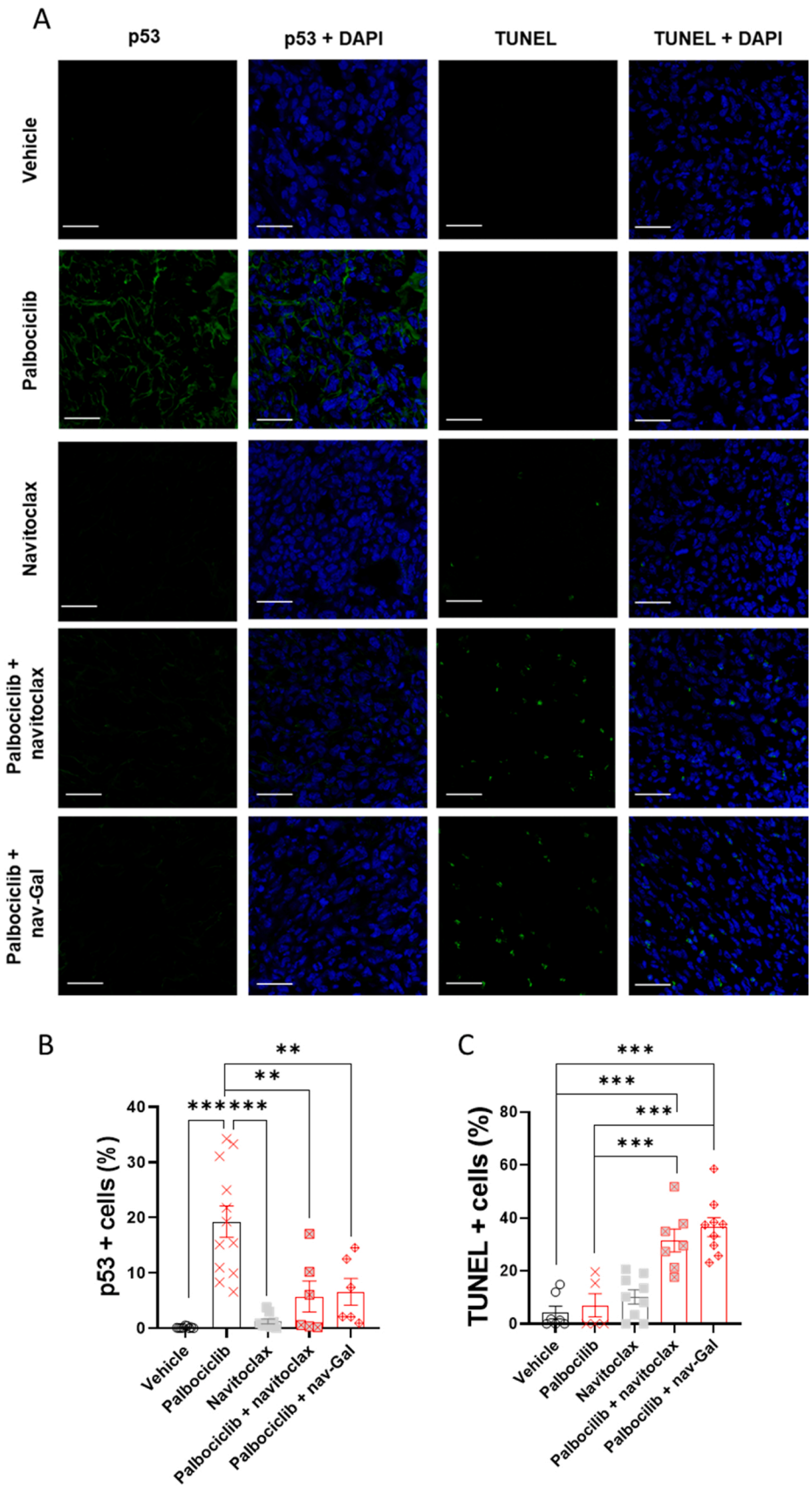

Fig. 4. Palbociclib and navitoclax co-treatment produces effective induction of senescence and cell death in tumors. (A) Representative confocal images of p53 immunostaining and TUNEL assay of tumor sections from animals treated with vehicle, palbociclib, navitoclax, or palbociclib and navitoclax or nav-Gal concomitantly ($n \geq 5$ tumors per group). TUNEL assay was used to confirm the induction of apoptosis in treated and untreated tumor tissues. Scale bar, 20 μm. (B) Percentage of p53- and (C) TUNEL-positive cells in tumors. Quantification was performed in a total of 3 fields per tumor, covering most of the whole tumor section. Data represent the mean ± SEM ($n = 5$), and statistical significance was assessed by one-way ANOVA followed by Tukey's post-tests (*$p < 0.05$; **$p < 0.01$; ***$p < 0.001$).

pharmacological induction of senescence, we used 5 μM palbociclib (#S1116, Selleckchem) for 7 days.

4.2. Senescence-associated β-galactosidase staining

Senescence-associated β-galactosidase detection was performed using the Senescence β-galactosidase Staining Kit (Cell Signaling, #9860 S). Briefly, cells were fixed at room temperature with 1x Fixative Solution, washed, and incubated overnight at 37 °C without CO_2 with fresh 1x Staining Solution containing X-gal in N-N-dimethylformamide. Cells were washed, visualized, and photographed under bright field microscope. For SA-β-Galactosidase staining in tumors, whole-mount tumor were fixed with 4% paraformaldehyde O/N. Then tumors were washed with PBS and incubated with X-Gal staining solution for 6 h at 37 °C.

4.3. Western blot

Cells were lysed in a buffer containing 25 mM Tris-HCl pH 7.4, 1 mM EDTA, 1% SDS, supplemented with protease and phosphatase inhibitors. Protein concentration was determined by the BCA protein assay. Electrophoresis was performed in SDS-PAGE gels, and proteins were transferred to nitrocellulose membranes. The membranes were blocked for 1 h with 5% non-fat milk, washed with 0.1% Tween/PBS and incubated with a specific primary antibody at 4 °C overnight. Membranes were washed and incubated with the corresponding secondary antibody conjugated with horseradish peroxidase. Membranes were visualized using ECL system (GE Healthcare) for chemiluminescent detection of the protein bands.

Antibodies: pRb (#9308, Cell Signaling), p53 (ab56, Abcam), Bcl-xL (#2764, Cell Signaling) Bcl-2 (#2870, Cell Signaling); Bcl-w (#2724, Cell Signaling); Mcl-1 (#4572, Cell signaling); Bak (#12105, Cell Signaling); Bax (#2772, Cell Signaling); Bok (ab186745, Abcam); Bim (#2819, Cell Signaling); Puma (#4976, Cell Signaling); Cdk4 (ab108357, Abcam); Cdk6 (ab124821, Abcam); tubulin (ab6160, Abcam); GADPH (#14C10, Cell Signalling); anti-Rabbit IgG peroxidase antibody (#A6154, Sigma) or peroxidase conjugate-goat anti-Mouse IgG antibody (#A4416, Sigma).

4.4. Ki67 immunostaining

Cells were seeded on coverslips; when cells were confluent, they were fixed with 4% PFA, permeabilized and blocked for 1 h with a solution containing 5% BSA and 0.3% Triton X-100. Then cells were stained with the primary antibody Ki-67 (D3B5) Rabbit (#9129, Cell Signaling) overnight at 4 °C. The following incubation with secondary antibody anti-rabbit IgG Fluor Goat 633 (#A21071, Fisher) was performed for 2 h at room temperature. The coverslips were mounted with Mowiol/DAPI (Sigma), and confocal microscopy images were taken using a Leica TCS SP8 HyVolution 2 microscope.

4.5. Cell cycle assay

For apoptosis evaluation assays, proliferating MDA-MB-231 and palbociclib-treated MDA-MB-231 cells (7 days at 5 μM) were fixed and permeabilized with ethanol overnight. Then, 0.5 mL of PI/RNAse buffer solution from Immunostep were added to each proliferating or senescent cells (1×10^6 cells) and incubated for 15 min at room temperature before analysis. Samples were analyzed by flow cytometry using the CytoFLEX S Beckman Coulter.

4.6. Synthesis of nav-Gal prodrug

Synthesis of nav-Gal was performed as described previously by González-Gualda et al. [23]. Briefly, in a round two neck bottom flask, 40 mg of navitoclax from Eurodiagnostico (0.04 mmol), 25 mg of 2,3,4,6-tetra-O-acetyl-α-D-galactopyranosyl-bromide from Sigma (0.06 mmol) and 10.5 mg of K_2CO_3 from Sigma (0.07 mmol) was added. The reaction mixture was purged with an argon atmosphere. Anhydrous acetonitrile (10 mL) was added, and the mixture was stirred at 70 °C for 3 h under an argon atmosphere. The solvent was removed under vacuum pressure. For large stocks used in mouse experiments, the reactions were performed in different batches. Once the desired amount was obtained, all batches were pooled and purified by column chromatography using silica gel (eluent, hexane-ethyl acetate (3:7 v/v; Scharlab) to hexane-ethyl acetate (7:3 v/v)). Purified nav-Gal was obtained as a yellow powder in 35% yield.

4.7. HPLC-MS characterization

Navitoclax (MedChemExpress) and nav-Gal were diluted in methanol at a concentration of 2 ppm and directly injected into HPLC-MS. Chromatograms were acquired after complete reaction (λ_{exc} = 365 nm) with an Agilent 1620 Infinity II high pressure liquid chromatography (HPLC) coupled to a mass spectrometer Agilent Ultivo equipped with a triple QTOF detector. Conditions: KromasilC18 column, 0.7 mL/min, (H_2O (0.1% acetic acid)): MeOH gradient elution: 50:50 0 min, 40:60 3 min, 30:70 10 min, 20:80 20 min, 10:90 25 min, 0:100 27 min

4.8. Cytotoxicity assay

Control proliferating and 7 days 5 μM palbociclib-induced senescent MDA-MB-231 cells were plated in white flat-bottom-clear 96-well (Greiner Bio-One) at a density of 10^4 cells per well. After 24 h, drugs (navitoclax, nav-Gal, S63845, ABT-199, WeHi-539 or A-1155463) (MedChemExpress) were added to the cells at a 20 μM final concentration. For simultaneous co-treatment of MDA-MB-231 cells with free palbociclib plus free navitoclax, after 24 h of the seeding, cells were treated with 5 μM palbociclib and 1.25 μM navitoclax. In all cases, after 72 h, viability was measured using CellTiter-Glo® luminescent cell viability assay (Promega, #G7571) kit following the manufacturer's instructions in a PerkinElmer life sciences wallac Victor2TM spectrophotometer. The number of viable cells was normalized to the internal control of untreated cells (DMSO only) of each plate. The senolytic index of the compounds was calculated by measuring the ratio of the half-maximal inhibitory concentration (IC50) values between control and senescent cells.

4.9. Cell death assay

For the apoptosis evaluation assay, senescent MDA-MB-231 cells were treated either with DMSO, navitoclax or nav-Gal 1 μM. After 48 h of incubation, cells were labelled with Alexa fluorescein isothiocyanate-conjugated Annexin V (BD Bioscience) plus propidium iodide according to the manufacturer's recommendations. Samples were analyzed in the cytometer CytoFLEX S Beckman Coulter.

4.10. Mouse experiments

All mice were treated in strict accordance with the local ethical committee (Ethical Committee for Research and Animal Welfare Generalitat Valenciana, Conselleria dÀgricultura, Medi ambient, Canvi climàtic i Desenvolupament Rural (2020/VSC/PEA/0177)). All mice were maintained in ventilated cages within a specific pathogen-free animal facility. To establish subcutaneous tumor xenografts, 2×10^6 MDA-MB-231 breast cancer cells were injected subcutaneously in the second lower right breast of 6–7 weeks old BALB/c nude mice. Tumors were measured with callipers every 2 days, and the tumor volume (mm^3) was calculated with the formula length × $width^2/2$. When tumor volume reached an average of 60 mm^3, daily therapy was initiated with either vehicle (sodium lactate) or 50 mg/kg palbociclib (*via* oral

gavage). The day after the initiation of palbociclib treatment, navitoclax treatments were initiated at a molar equivalent dose: either 25 mg/kg navitoclax (*via* oral gavage) or 33.5 mg/kg nav-Gal (*via* i.p. injection). Navitoclax was prepared in 15% DMSO/ 85% PEG-400 while nav-Gal was prepared in 10% DMSO/ 90% saline. Mice were culled by CO_2 after 20 days of treatment, and tumors and lungs were collected for subsequent histological analyses.

4.11. Histology

Tumors were removed, washed with 1 × PBS, and fixed with 4% PFA overnight at 4 °C. The fixative was aspirated, the tumor was washed in 1 × PBS and incubated with 30% sucrose overnight at 4 °C. Fixed tissues were embedded in cryomolds with OCT and frozen completely at − 20 °C. 10 μm thick tumor sections were then incubated in blocking solution (5% horse serum, 0.3% Triton X-100 in 1 × PBS) for 1 h and immunostained following incubation with primary antibodies overnight at 4 °C. p53 antibody was used at 1:100 (ab26, Abcam). Secondary antibody against mouse conjugated to Alexa Fluor 488 (Invitrogen) 1:200 dilution. For TUNEL staining, In Situ Cell Death Detection Kit (Merck) was used as per manufacturer's instructions. Sections were mounted on microscope slides using the Mowiol/DAPI (Sigma) and covered with a glass coverslip. Confocal microscopy images were obtained by using a Leica TCS SP8 HyVolution 2 microscope. Positive signal for p53 and TUNEL was quantified with ImageJ or Aperio Versa software.

4.12. Metastasis quantification

Lungs were collected after euthanasia and fixed overnight in 4% PFA. Paraffin-embedded tissue Section (5 μm) on glass slides were processed for haematoxylin-eosin staining, and stained lung sections were scanned in a Leica Aperio Versa 200 equipment at 10x magnification. Metastatic MDA-MB-231 cell clusters were microscopically counted in different lung sections from five animals per group.

4.13. Statistical analysis

For *in vivo* studies, mice were randomly assigned to treatment groups. All of the values represent the mean ± SEM of at least three independent experiments except the *in vivo* experiment with mice where a single representative experiment is shown. Significance was determined by one-way ANOVA followed by either Tukey's post-tests or Sidak's post-tests or by Student's T-test using GraphPad Prism 8 software. A p-value below 0.05 was considered statistically significant ($^*p < 0.05$; $^{**}p < 0.01$; $^{***}p < 0.001$).

Ethics approval and consent to participate

The study was approved by the Ethical Committee for Research and Animal Welfare Generalitat Valenciana, Conselleria dÀgricultura, Medi ambient, Canvi climàtic i Desenvolupament Rural (2020/VSC/PEA/0177).

CRediT authorship contribution statement

A.E-F performed most of the experiments and contributed to the experimental design, data analysis, discussion and writing. A.G.-F performed cell cycle experiment and helped with experimental design, data analysis, discussion and writing. A.L.-V helped with *in vitro* and *in vivo* experiments, data analysis and discussion. J.F.B. synthetized the prodrug. I.G. performed Bcl-2 protein family western blot. M.O. supervised the biological studies and contributed to discussion and writing. R.M.-M. and F.S. supervised the chemical synthesis of the prodrug and contributed to discussion and writing. All authors revised and commented on the manuscript.

Declaration of Competing Interest

Not applicable.

Availability of data and material

Further information and requests for resources and reagents should be directed to and will be fulfilled by the lead contact, R.M-M. (rmaez@quim.upv.es).

Acknowledgments

This work was supported by the Spanish Government projects (RTI2018–100910-B-C41, RTI2018–101599-B-C22 and PID2020–115048RB-I00 (MCUI/FEDER, EU)) and the Generalitat Valenciana (PROMETEO 2018/024 and PROMETEO/2019/065). A.E-F. is grateful to the Spanish Government for her Ph.D. grant (FPU17/05454), A.L-V. is grateful to the Instituto de Salud Carlos III for her Ph.D. i-PFIS grant (IFI17/00039). J.B. thanks to the Instituto de Salud Carlos III for his Sara Borrell contract (CD19/00038). Thank the financial support from the FEDER found of European Union (IDIFEDER/2021/044). The authors thank Alberto Hernández for the confocal microscope, Alicia Martinez for flow cytometry, and Viviana Bisbal for veterinary assistance. The authors thank for the use of Biorender.com in the graphical abstract Fig. 2 and Fig. 3.

Appendix A. Supporting information

Supplementary data associated with this article can be found in the online version at doi:10.1016/j.phrs.2022.106628.

References

[1] G.J. Morris, S. Naidu, A.K. Topham, F. Guiles, Y. Xu, P. McCue, G.F. Schwartz, P. K. Park, A.L. Rosenberg, K. Brill, E.P. Mitchell, Differences in breast carcinoma characteristics in newly diagnosed African-American and Caucasian patients: A single-institution compilation compared with the national cancer institute's surveillance, epidemiology, and end results database, Cancer 110 (2007) 876–884, https://doi.org/10.1002/cncr.22836.

[2] P. Boix-Montesinos, P.M. Soriano-Teruel, A. Armiñán, M. Orzáez, M.J. Vicent, The past, present, and future of breast cancer models for nanomedicine development, Adv. Drug Deliv. Rev. 173 (2021) 306–330, https://doi.org/10.1016/j.addr.2021.03.018.

[3] A.C. Wolff, M.E.H. Hammond, D.G. Hicks, M. Dowsett, L.M. McShane, K.H. Allison, D.C. Allred, J.M.S. Bartlett, M. Bilous, P. Fitzgibbons, W. Hanna, R.B. Jenkins, P. B. Mangu, S. Paik, E.A. Perez, M.F. Press, P.A. Spears, G.H. Vance, G. Viale, D. F. Hayes, Recommendations for human epidermal growth factor receptor 2 testing in breast, J. Clin. Oncol. 31 (2013) 3997–4013, https://doi.org/10.1200/JCO.2013.50.9984.

[4] F. Cardoso, S. Paluch-Shimon, E. Senkus, G. Curigliano, M.S. Aapro, F. André, C. H. Barrios, J. Bergh, G.S. Bhattacharyya, L. Biganzoli, F. Boyle, M.-J. Cardoso, L. A. Carey, J. Cortés, N.S. El Saghir, M. Elzayat, A. Eniu, L. Fallowfield, P.A. Francis, K. Gelmon, J. Gligorov, R. Haidinger, N. Harbeck, X. Hu, B. Kaufman, R. Kaur, B. E. Kiely, S.-B. Kim, N.U. Lin, S.A. Mertz, S. Neciosup, B.V. Offersen, S. Ohno, O. Pagani, A. Prat, F. Penault-Llorca, H.S. Rugo, G.W. Sledge, C. Thomssen, D. A. Vorobiof, T. Wiseman, B. Xu, L. Norton, A. Costa, E.P. Winer, 5th ESO-ESMO international consensus guidelines for advanced breast cancer (ABC 5), Ann. Oncol. 31 (2020) 1623, https://doi.org/10.1016/J.ANNONC.2020.09.010.

[5] A.C. Garrido-Castro, N.U. Lin, K. Polyak, Insights into molecular classifications of triple-negative breast cancer: Improving patient selection for treatment, Cancer Disco 9 (2019) 176–198, https://doi.org/10.1158/2159-8290.CD-18-1177.

[6] I. Galiana, B. Lozano-Torres, M. Sancho, M. Alfonso, A. Bernardos, V. Bisbal, M. Serrano, R. Martínez-Máñez, M. Orzáez, Preclinical antitumor efficacy of senescence-inducing chemotherapy combined with a nanoSenolytic, J. Control. Release 323 (2020) 624–634, https://doi.org/10.1016/j.jconrel.2020.04.045.

[7] T. Saleh, V.J. Carpenter, L. Tyutyunyk-Massey, G. Murray, J.D. Leverson, A. J. Souers, M.R. Alotaibi, A.C. Faber, J. Reed, H. Harada, D.A. Gewirtz, Clearance of therapy-induced senescent tumor cells by the senolytic ABT-263 via interference with BCL-XL–BAX interaction, Mol. Oncol. 14 (2020) 2504–2519, https://doi.org/10.1002/1878-0261.12761.

[8] D. Muñoz-Espín, M. Rovira, I. Galiana, C. Giménez, B. Lozano-Torres, M. Paez-Ribes, S. Llanos, S. Chaib, M. Muñoz-Martín, A.C. Ucero, G. Garaulet, F. Mulero, S. G. Dann, T. VanArsdale, D.J. Shields, A. Bernardos, J.R. Murguía, R. Martínez-Máñez, M. Serrano, A versatile drug delivery system targeting senescent cells, EMBO Mol. Med. 10 (2018), https://doi.org/10.15252/emmm.201809355.

[9] A. Estepa-Fernández, M. Alfonso, Á. Morellá-Aucejo, A. García-Fernández, A. Lérida-Viso, B. Lozano-Torres, I. Galiana, P.M. Soriano-Teruel, F. Sancenón, M. Orzáez, R. Martínez-Máñez, Senolysis reduces senescence in veins and cancer cell migration, Adv. Ther. 2100149 (2021) 1–15, https://doi.org/10.1002/adtp.202100149.

[10] J.A. Beaver, L. Amiri-Kordestani, R. Charlab, W. Chen, T. Palmby, A. Tilley, J. F. Zirkelbach, J. Yu, Q. Liu, L. Zhao, J. Crich, X.H. Chen, M. Hughes, E. Bloomquist, S. Tang, R. Sridhara, P.G. Kluetz, G. Kim, A. Ibrahim, R. Pazdur, P. Cortazar, FDA Approval: Palbociclib for the treatment of postmenopausal patients with estrogen receptor-positive, HER2-negative metastatic breast cancer, Clin. Cancer Res. 21 (2015) 4760–4766, https://doi.org/10.1158/1078-0432.CCR-15-1185.

[11] A.J. Walker, S. Wedam, L. Amiri-Kordestani, E. Bloomquist, S. Tang, R. Sridhara, W. Chen, T.R. Palmby, J. Fourie Zirkelbach, W. Fu, Q. Liu, A. Tilley, G. Kim, P. G. Kluetz, A.E. McKee, R. Pazdur, FDA Approval of palbociclib in combination with fulvestrant for the treatment of hormone receptor-positive, HER2-negative metastatic breast cancer, Clin. Cancer Res. 22 (2016) 4968–4972, https://doi.org/10.1158/1078-0432.CCR-16-0493.

[12] S. Wedam, L. Fashoyin-Aje, E. Bloomquist, S. Tang, R. Sridhara, K.B. Goldberg, M. R. Theoret, L. Amiri-Kordestani, R. Pazdur, J.A. Beaver, FDA approval summary: palbociclib for male patients with metastatic breast cancer, Clin. Cancer Res. 26 (2019), https://doi.org/10.1158/1078-0432.ccr-19-2580.

[13] Y. Huang, H. Wu, X. Li, Novel sequential treatment with palbociclib enhances the effect of cisplatin in RB-proficient triple-negative breast cancer, Cancer Cell Int. 20 (2020) 1–14, https://doi.org/10.1186/s12935-020-01597-x.

[14] M. Demaria, M.N. O'Leary, J. Chang, L. Shao, S. Liu, F. Alimirah, K. Koenig, C. Le, N. Mitin, A.M. Deal, S. Alston, E.C. Academia, S. Kilmarx, A. Valdovinos, B. Wang, A. De Bruin, B.K. Kennedy, S. Melov, D. Zhou, N.E. Sharpless, H. Muss, J. Campisi, Cellular senescence promotes adverse effects of chemotherapy and cancer relapse, Cancer Disco 7 (2017) 165–176, https://doi.org/10.1158/2159-8290.CD-16-0241.

[15] T. Saleh, L. Tyutynuk-Massey, E.K.J. Cudjoe, M.O. Idowu, J.W. Landry, D. A. Gewirtz, Non-cell autonomous effects of the senescence-associated secretory phenotype in cancer therapy, Front. Oncol. 0 (2018) 164, https://doi.org/10.3389/FONC.2018.00164.

[16] H.-N.N. Kim, J. Chang, L. Shao, L. Han, S. Iyer, S.C. Manolagas, C.A. O'Brien, R. L. Jilka, D. Zhou, M. Almeida, DNA damage and senescence in osteoprogenitors expressing Osx1 may cause their decrease with age, Aging Cell 16 (2017) 693–703, https://doi.org/10.1111/acel.12597.

[17] J. Chang, Y. Wang, L. Shao, R.M. Laberge, M. Demaria, J. Campisi, K. Janakiraman, N.E. Sharpless, S. Ding, W. Feng, Y. Luo, X. Wang, N. Aykin-Burns, K. Krager, U. Ponnappan, M. Hauer-Jensen, A. Meng, D. Zhou, Clearance of senescent cells by ABT263 rejuvenates aged hematopoietic stem cells in mice, Nat. Med. 22 (2016) 78–83, https://doi.org/10.1038/nm.4010.

[18] T.J. Bussian, A. Aziz, C.F. Meyer, B.L. Swenson, J.M. van Deursen, D.J. Baker, Clearance of senescent glial cells prevents tau-dependent pathology and cognitive decline, Nature 562 (2018) 578–582, https://doi.org/10.1038/s41586-018-0543-y.

[19] Y. Zhu, T. Tchkonia, H. Fuhrmann-Stroissnigg, H.M. Dai, Y.Y. Ling, M.B. Stout, T. Pirtskhalava, N. Giorgadze, K.O. Johnson, C.B. Giles, J.D. Wren, L. J. Niedernhofer, P.D. Robbins, J.L. Kirkland, Identification of a novel senolytic agent, navitoclax, targeting the Bcl-2 family of anti-apoptotic factors, Aging Cell 15 (2016) 428–435, https://doi.org/10.1111/acel.12445.

[20] R. Yosef, N. Pilpel, R. Tokarsky-Amiel, A. Biran, Y. Ovadya, S. Cohen, E. Vadai, L. Dassa, E. Shahar, R. Condiotti, I. Ben-Porath, V. Krizhanovsky, Directed elimination of senescent cells by inhibition of BCL-W and BCL-XL, Nat. Commun. 7 (2016) 1–11, https://doi.org/10.1038/ncomms11190.

[21] S.M. Schoenwaelder, K.E. Jarman, E.E. Gardiner, M. Hua, J. Qiao, M.J. White, E. C. Josefsson, I. Alwis, A. Ono, A. Willcox, R.K. Andrews, K.D. Mason, H.H. Salem, D.C.S. Huang, B.T. Kile, A.W. Roberts, S.P. Jackson, Bcl-xL-inhibitory BH3 mimetics can induce a transient thrombocytopathy that undermines the hemostatic function of platelets, Blood 118 (2011) 1663–1674, https://doi.org/10.1182/BLOOD-2011-04-347849.

[22] B.T. Kile, The role of apoptosis in megakaryocytes and platelets, Br. J. Haematol. 165 (2014) 217–226, https://doi.org/10.1111/bjh.12757.

[23] E. González-Gualda, M. Pàez-Ribes, B. Lozano-Torres, D. Macias, J.R. Wilson, C. González-López, H.L. Ou, S. Mirón-Barroso, Z. Zhang, A. Lérida-Viso, J. F. Blandez, A. Bernardos, F. Sancenón, M. Rovira, L. Fruk, C.P. Martins, M. Serrano, G.J. Doherty, R. Martínez-Máñez, D. Muñoz-Espín, Galacto-conjugation of Navitoclax as an efficient strategy to increase senolytic specificity and reduce platelet toxicity, Aging Cell 19 (2020) 1–19, https://doi.org/10.1111/acel.13142.

[24] B. Lozano-Torres, I. Galiana, M. Rovira, E. Garrido, S. Chaib, A. Bernardos, D. Muñoz-Espín, M. Serrano, R. Martínez-Máñez, F. Sancenón, An OFF–ON Two-Photon Fluorescent Probe for Tracking Cell Senescence *in Vivo*, J. Am. Chem. Soc. 139 (2017) 8808–8811, https://doi.org/10.1021/jacs.7b04985.

[25] B. Lozano-Torres, J.F. Blandez, I. Galiana, J.A. Lopez-Dominguez, M. Rovira, M. Paez-Ribes, E. González-Gualda, D. Muñoz-Espín, M. Serrano, F. Sancenón, R. Martínez-Máñez, A. Two-Photon Probe Based, on Naphthalimide-Styrene Fluorophore for the in Vivo Tracking of Cellular Senescence, Anal. Chem. 93 (2021) 3052–3060, https://doi.org/10.1021/acs.analchem.0c05447.

[26] S. Goel, M.J. DeCristo, S.S. McAllister, J.J. Zhao, CDK4/6 Inhibition in cancer: beyond cell cycle arrest, Trends Cell Biol. 28 (2018) 911–925, https://doi.org/10.1016/j.tcb.2018.07.002.

[27] G. Vivo-Llorca, V. Candela-Noguera, M. Alfonso, A. García-Fernández, M. Orzáez, F. Sancenón, R. Martínez-Máñez, M.U.C.1 Aptamer-Capped Mesoporous, Silica nanoparticles for navitoclax resistance overcoming in triple-negative breast cancer, Chem. - A Eur. J. 26 (2020) 16318–16327, https://doi.org/10.1002/chem.202001579.

[28] L. Yin, J.J. Duan, X.W. Bian, S.C. Yu, Triple-negative breast cancer molecular subtyping and treatment progress, Breast Cancer Res 22 (2020) 1–13, https://doi.org/10.1186/s13058-020-01296-5.

[29] D. O'Reilly, M. Al Sendi, C.M. Kelly, Overview of recent advances in metastatic triple negative breast cancer, World J. Clin. Oncol. 12 (2021) 164–182, https://doi.org/10.5306/wjco.v12.i3.164.

[30] R. Dent, M. Trudeau, K.I. Pritchard, W.M. Hanna, H.K. Kahn, C.A. Sawka, L. A. Lickley, E. Rawlinson, P. Sun, S.A. Narod, Triple-negative breast cancer: clinical features and patterns of recurrence, Clin. Cancer Res 13 (2007) 4429–4434, https://doi.org/10.1158/1078-0432.CCR-06-3045.

[31] L. Wang, L. Lankhorst, R. Bernards, Exploiting senescence for the treatment of cancer, Nat. Rev. Cancer 2022 (2022) 1–16, https://doi.org/10.1038/s41568-022-00450-9.

[32] S. Short, E. Fielder, S. Miwa, T. von Zglinicki, Senolytics and senostatics as adjuvant tumour therapy, EBioMedicine 41 (2019) 683–692, https://doi.org/10.1016/J.EBIOM.2019.01.056.

[33] P.G. Prasanna, D.E. Citrin, J. Hildesheim, M.M. Ahmed, S. Venkatachalam, G. Riscuta, D. Xi, G. Zheng, J. Van Deursen, J. Goronzy, S.J. Kron, M.S. Anscher, N. E. Sharpless, J. Campisi, S.L. Brown, L.J. Niedernhofer, A. O'loghlen, A. G. Georgakilas, F. Paris, D. Gius, D.A. Gewirtz, C.A. Schmitt, M.E. Abazeed, J. L. Kirkland, A. Richmond, P.B. Romesser, S.W. Lowe, J. Gil, M.S. Mendonca, S. Burma, D. Zhou, C.N. Coleman, Therapy-induced senescence: opportunities to improve anticancer therapy, JNCI J. Natl. Cancer Inst. 113 (2021) 64, https://doi.org/10.1093/jnci/djab064.

[34] S.S. Park, Y.W. Choi, J.H. Kim, H.S. Kim, T.J. Park, Senescent tumor cells: an overlooked adversary in the battle against cancer, 2021, Exp. Mol. Med 5312 (53) (2021) 1834–1841, https://doi.org/10.1038/s12276-021-00717-5.

[35] M.P. Mongiardi, M. Pellegrini, R. Pallini, A. Levi, M.L. Falchetti, Cancer response to therapy-induced senescence: a matter of dose and timing, 13 (2021) 484, Cancers Vol. 13 (2021) 484, https://doi.org/10.3390/CANCERS13030484.

[36] B. Wang, J. Kohli, M. Demaria, Senescent cells in cancer therapy: friends or foes, Trends Cancer 6 (2020) 838–857, https://doi.org/10.1016/j.trecan.2020.05.004.

[37] L. Wyld, I. Bellantuono, T. Tchkonia, J. Morgan, O. Turner, F. Foss, J. George, S. Danson, J.L. Kirkland, Senescence and cancer: a review of clinical implications of senescence and senotherapies, Cancers (Basel) 12 (2020) 1–20, https://doi.org/10.3390/cancers12082134.

[38] B.D. Chang, E.V. Broude, M. Dokmanovic, H. Zhu, A. Ruth, Y. Xuan, E.S. Kandel, E. Lausch, K. Christov, I.B. Roninson, A senescence-like phenotype distinguishes tumor cells that undergo terminal proliferation arrest after exposure to anticancer agents, Cancer Res 59 (1999) 3761–3767.

[39] R.H. te Poele, A.L. Okorokov, L. Jardine, J. Cummings, S.P. Joel, DNA damage is able to induce senescence in tumor cells in vitro and in vivo, Cancer Res 62 (2002) 1876–1883.

[40] X. Wang, S.C. Wong, J. Pan, S.W. Tsao, K.H. Fung, D.L. Kwong, J.S. Sham, J. M. Nicholls, Evidence of cisplatin-induced senescent-like growth arrest in nasopharyngeal carcinoma cells, Cancer Res 58 (1998) 5019–5022.

[41] Y. Hirose, M.S. Berger, R.O. Pieper, p53 effects both the duration of G2/M arrest and the fate of temozolomide-treated human glioblastoma cells, Cancer Res 61 (2001) 1957–1963.

[42] R. Torres-Guzmán, B. Calsina, A. Hermoso, C. Baquero, B. Alvarez, J. Amat, A. M. McNulty, X. Gong, K. Boehnke, J. Du, A. de Dios, R.P. Beckmann, S. Buchanan, M.J. Lallena, Preclinical characterization of abemaciclib in hormone receptor positive breast cancer, Oncotarget 8 (2017) 69493, https://doi.org/10.18632/ONCOTARGET.17778.

[43] R. Bortolozzi, E. Mattiuzzo, L. Trentin, B. Accordi, G. Basso, G. Viola, Ribociclib, a Cdk4/Cdk6 kinase inhibitor, enhances glucocorticoid sensitivity in B-acute lymphoblastic leukemia (B-All, Biochem. Pharmacol. 153 (2018) 230–241, https://doi.org/10.1016/J.BCP.2018.01.050.

[44] A. Yoshida, E.K. Lee, J.A. Diehl, Induction of therapeutic senescence in vemurafenib-resistant melanoma by extended inhibition of CDK4/6, Cancer Res 76 (2016) 2990–3002, https://doi.org/10.1158/0008-5472.CAN-15-2931/652215/AM/INDUCTION-OF-THERAPEUTIC-SENESCENCE-IN-VEMURAFENIB.

[45] C.A. Valenzuela, L. Vargas, V. Martinez, S. Bravo, N.E. Brown, Palbociclib-induced autophagy and senescence in gastric cancer cells, Exp. Cell Res. 360 (2017) 390–396, https://doi.org/10.1016/J.YEXCR.2017.09.031.

[46] M.K. Ruhland, L.M. Coussens, S.A. Stewart, Senescence and cancer: an evolving inflammatory paradox, Biochim. Biophys. Acta - Rev. Cancer 1865 (2016) 14–22, https://doi.org/10.1016/j.bbcan.2015.10.001.

[47] T.-W. Kang, T. Yevsa, N. Woller, L. Hoenicke, T. Wuestefeld, D. Dauch, A. Hohmeyer, M. Gereke, R. Rudalska, A. Potapova, M. Iken, M. Vucur, S. Weiss, M. Heikenwalder, S. Khan, J. Gil, D. Bruder, M. Manns, P. Schirmacher, F. Tacke, M. Ott, T. Luedde, T. Longerich, S. Kubicka, L. Zender, Senescence surveillance of pre-malignant hepatocytes limits liver cancer development, Nature 479 (2011) 547–551, https://doi.org/10.1038/nature10599.

[48] J.-P. Coppé, P.-Y. Desprez, A. Krtolica, J. Campisi, The senescence-associated secretory phenotype: the dark side of tumor suppression, Annu. Rev. Pathol. Mech. Dis. 5 (2010) 99–118, https://doi.org/10.1146/annurev-pathol-121808-102144.

[49] T. Eggert, K. Wolter, J. Ji, C. Ma, T. Yevsa, S. Klotz, J. Medina-Echeverz, T. Longerich, M. Forgues, F. Reisinger, M. Heikenwalder, X.W. Wang, L. Zender, T. F. Greten, Distinct functions of senescence-associated immune responses in liver tumor surveillance and tumor progression, Cancer Cell 30 (2016) 533–547, https://doi.org/10.1016/j.ccell.2016.09.003.

[50] R.S. Roberson, S.J. Kussick, E. Vallieres, S.Y.J. Chen, D.Y. Wu, Escape from therapy-induced accelerated cellular senescence in p53-null lung cancer cells and in human lung cancers, Cancer Res 65 (2005) 2795–2803, https://doi.org/10.1158/0008-5472.CAN-04-1270.

[51] Y. Yu, H. Liao, R. Xie, Y. Zhang, R. Zheng, J. Chen, B. Zhang, Overexpression of miRNA-3613-3p Enhances the Sensitivity of Triple Negative Breast Cancer to CDK4/6 Inhibitor Palbociclib, Front. Oncol. 10 (2020) 1–14, https://doi.org/10.3389/fonc.2020.590813.
[52] F. Triana-Martínez, M.I. Loza, E. Domínguez, Beyond tumor suppression: senescence in cancer stemness and tumor dormancy, Cells 9 (2020), https://doi.org/10.3390/cells9020346.
[53] T. Saleh, L. Tyutyunyk-Massey, G.F. Murray, M.R. Alotaibi, A.S. Kawale, Z. Elsayed, S.C. Henderson, V. Yakovlev, L.W. Elmore, A. Toor, H. Harada, J. Reed, J.W. Landry, D.A. Gewirtz, Tumor cell escape from therapy-induced senescence, Biochem. Pharmacol. 162 (2019) 202–212, https://doi.org/10.1016/j.bcp.2018.12.013.
[54] T. Saleh, L. Tyutyunyk-Massey, D.A. Gewirtz, Tumor cell escape from therapy-induced senescence as a model of disease recurrence after dormancy, Cancer Res 79 (2019) 1044–1046, https://doi.org/10.1158/0008-5472.CAN-18-3437.
[55] B. Lozano-Torres, A. Estepa-Fernández, M. Rovira, M. Orzáez, M. Serrano, R. Martínez-Máñez, F. Sancenón, The chemistry of senescence, Nat. Rev. Chem. 3 (2019) 426–441, https://doi.org/10.1038/s41570-019-0108-0.
[56] J.N. Justice, A.M. Nambiar, T. Tchkonia, N.K. LeBrasseur, R. Pascual, S.K. Hashmi, L. Prata, M.M. Masternak, S.B. Kritchevsky, N. Musi, J.L. Kirkland, Senolytics in idiopathic pulmonary fibrosis: Results from a first-in-human, open-label, pilot study, EBioMedicine 40 (2019) 554–563, https://doi.org/10.1016/J.EBIOM.2018.12.052.
[57] L.T.J. Hickson, L.G.P. Langhi Prata, S.A. Bobart, T.K. Evans, N. Giorgadze, S. K. Hashmi, S.M. Herrmann, M.D. Jensen, Q. Jia, K.L. Jordan, T.A. Kellogg, S. Khosla, D.M. Koerber, A.B. Lagnado, D.K. Lawson, N.K. LeBrasseur, L.O. Lerman, K.M. McDonald, T.J. McKenzie, J.F. Passos, R.J. Pignolo, T. Pirtskhalava, I. M. Saadiq, K.K. Schaefer, S.C. Textor, S.G. Victorelli, T.L. Volkman, A. Xue, M. A. Wentworth, E.O. Wissler Gerdes, Y. Zhu, T. Tchkonia, J.L. Kirkland, Senolytics decrease senescent cells in humans: Preliminary report from a clinical trial of Dasatinib plus Quercetin in individuals with diabetic kidney disease, EBioMedicine 47 (2019) 446–456, https://doi.org/10.1016/J.EBIOM.2019.08.069.
[58] C. Tse, A.R. Shoemaker, J. Adickes, M.G. Anderson, J. Chen, S. Jin, E.F. Johnson, K. C. Marsh, M.J. Mitten, P. Nimmer, L. Roberts, S.K. Tahir, Y. Xiao, X. Yang, H. Zhang, S. Fesik, S.H. Rosenberg, S.W. Elmore, ABT-263: a potent and orally bioavailable Bcl-2 family inhibitor, Cancer Res 68 (2008) 3421–3428, https://doi.org/10.1158/0008-5472.CAN-07-5836.
[59] A.R. Shoemaker, M.J. Mitten, J. Adickes, S. Ackler, M. Refici, D. Ferguson, A. Oleksijew, J.M. O'Connor, B. Wang, D.J. Frost, J. Bauch, K. Marsh, S.K. tahir, X. Yang, C. Tse, S.W. Fesik, S.H. Rosenberg, S.W. Elmore, Activity of the Bcl-2 family inhibitor ABT-263 in a panel of small cell lung cancer xenograft models, Clin. Cancer Res 14 (2008) 3268–3277, https://doi.org/10.1158/1078-0432.CCR-07-4622.
[60] J. Chen, S. Jin, V. Abraham, X. Huang, B. Liu, M.J. Mitten, P. Nimmer, X. Lin, M. Smith, Y. Shen, A.R. Shoemaker, S.K. Tahir, H. Zhang, S.L. Ackler, S. H. Rosenberg, H. Maecker, D. Sampath, J.D. Leverson, C. Tse, S.W. Elmore, The Bcl-2/Bcl-X L/Bcl-w inhibitor, navitoclax, enhances the activity of chemotherapeutic agents in vitro and in vivo, Mol. Cancer Ther. 10 (2011) 2340–2349, https://doi.org/10.1158/1535-7163.MCT-11-0415.
[61] A. Shahbandi, S.G. Rao, A.Y. Anderson, W.D. Frey, J.O. Olayiwola, N. A. Ungerleider, J.G. Jackson, BH3 mimetics selectively eliminate chemotherapy-induced senescent cells and improve response in TP53 wild-type breast cancer, Cell Death Differ. 27 (2020) 3097–3116, https://doi.org/10.1038/s41418-020-0564-6.
[62] H. Fleury, N. Malaquin, V. Tu, S. Gilbert, A. Martinez, M.A. Olivier, A. Sauriol, L. Communal, K. Leclerc-Desaulniers, E. Carmona, D. Provencher, A.M. Mes-Masson, F. Rodier, Exploiting interconnected synthetic lethal interactions between PARP inhibition and cancer cell reversible senescence, 2019, Nat. Commun. 101 (10) (2019) 1–15, https://doi.org/10.1038/s41467-019-10460-1.
[63] M. Paez-Ribes, E. González-Gualda, G.J. Doherty, D. Muñoz-Espín, Targeting senescent cells in translational medicine, EMBO Mol. Med. 11 (2019) 1–19, https://doi.org/10.15252/emmm.201810234.
[64] P.L. Toogood, P.J. Harvey, J.T. Repine, D.J. Sheehan, S.N. VanderWel, H. Zhou, P. R. Keller, D.J. McNamara, D. Sherry, T. Zhu, J. Brodfuehrer, C. Choi, M.R. Barvian, D.W. Fry, Discovery of a potent and selective inhibitor of cyclin-dependent kinase 4/6, J. Med. Chem. 48 (2005) 2388–2406, https://doi.org/10.1021/JM049354H/SUPPL_FILE/JM049354HSI20050107_011813.PDF.
[65] L.M. Gelbert, S. Cai, X. Lin, C. Sanchez-Martinez, M. Del Prado, M.J. Lallena, R. Torres, R.T. Ajamie, G.N. Wishart, R.S. Flack, B.L. Neubauer, J. Young, E. M. Chan, P. Iversen, D. Cronier, E. Kreklau, A. De Dios, Preclinical characterization of the CDK4/6 inhibitor LY2835219: in-vivo cell cycle-dependent/independent anti-tumor activities alone/in combination with gemcitabine, Invest. N. Drugs 32 (2014) 825–837, https://doi.org/10.1007/S10637-014-0120-7.
[66] Z. Ouyang, S. Wang, M. Zeng, Z. Li, Q. Zhang, W. Wang, T. Liu, Therapeutic effect of palbociclib in chondrosarcoma: Implication of cyclin-dependent kinase 4 as a potential target, Cell Commun. Signal. 17 (2019), https://doi.org/10.1186/S12964-019-0327-5.
[67] K. Pandey, H.J. An, S.K. Kim, S.A. Lee, S. Kim, S.M. Lim, G.M. Kim, J. Sohn, Y. W. Moon, Molecular mechanisms of resistance to CDK4/6 inhibitors in breast cancer: A review, Int. J. Cancer 145 (2019) 1179, https://doi.org/10.1002/IJC.32020.
[68] D.B. Rivadeneira, C.N. Mayhew, C. Thangavel, E. Sotillo, C.A. Reed, X. Graña, E. S. Knudsen, Proliferative suppression by CDK4/6 inhibition: complex function of the retinoblastoma pathway in liver tissue and hepatoma cells, Gastroenterology 138 (2010), https://doi.org/10.1053/j.gastro.2010.01.007.
[69] C. Zeng, W. Shang, K. Wang, C. Chi, X. Jia, C. Feng, D. Yang, J. Ye, C. Fang, J. Tian, Intraoperative identification of liver cancer microfoci using a targeted near-infrared fluorescent probe for imaging-guided surgery, Sci. Rep. 6 (2016) 1–10, https://doi.org/10.1038/srep21959.
[70] A. Llombart-Cussac, J.M. Pérez-García, M. Bellet, F. Dalenc, M. Gil-Gil, M. Ruíz-Borrego, J. Gavilá, M. Sampayo-Cordero, E. Aguirre, P. Schmid, F. Marmé, S. Di Cosimo, J. Gligorov, A. Schneeweiss, J. Albanell, P. Zamora, D. Wheatley, E. Martínez-De Dueñas, K. Amillano, A. Malfettone, J. Cortés, Fulvestrant-palbociclib vs letrozole-palbociclib as initial therapy for endocrine-sensitive, hormone receptor-positive, erbb2-negative advanced breast cancer: a randomized clinical trial, JAMA Oncol. 7 (2021) 1791–1799, https://doi.org/10.1001/JAMAONCOL.2021.4301.
[71] H.S. Rugo, R.S. Finn, V. Diéras, J. Ettl, O. Lipatov, A.A. Joy, N. Harbeck, A. Castrellon, S. Iyer, D.R. Lu, A. Mori, E.R. Gauthier, C.H. Bartlett, K.A. Gelmon, D. J. Slamon, Palbociclib plus letrozole as first-line therapy in estrogen receptor-positive/human epidermal growth factor receptor 2-negative advanced breast cancer with extended follow-up, Breast Cancer Res. Treat. 174 (2019) 719–729, https://doi.org/10.1007/S10549-018-05125-4/FIGURES/4.
[72] C.Y. Liu, K.Y. Lau, C.C. Hsu, J.L. Chen, C.H. Lee, T.T. Huang, Y.T. Chen, C. T. Huang, P.H. Lin, L.M. Tseng, Combination of palbociclib with enzalutamide shows in vitro activity in RB proficient and androgen receptor positive triple negative breast cancer cells, PLoS One 12 (2017) 1–14, https://doi.org/10.1371/journal.pone.0189007.
[73] B.L. Bryson, I. Tamagno, S.E. Taylor, N. Parameswaran, N.M. Chernosky, N. Balasubramaniam, M.W. Jackson, Aberrant induction of a mesenchymal/stem cell program engages senescence in normal mammary epithelial cells, Mol. Cancer Res. 19 (2021) 651–666, https://doi.org/10.1158/1541-7786.MCR-19-1181.
[74] T. Jost, L. Heinzerling, R. Fietkau, M. Hecht, L.V. Distel, Palbociclib induces senescence in melanoma and breast cancer cells and leads to additive growth arrest in combination with irradiation, Front. Oncol. 11 (2021) 4059, https://doi.org/10.3389/FONC.2021.740002/BIBTEX.
[75] N.S. Nor Hisam, A. Ugusman, N.F. Rajab, M.F. Ahmad, M. Fenech, S.L. Liew, N.N. Mohamad Anuar, Combination therapy of navitoclax with chemotherapeutic agents in solid tumors and blood cancer: a review of current evidence, Pharmaceutics 13 (2021), https://doi.org/10.3390/pharmaceutics13091353.
[76] A. Kaefer, J. Yang, P. Noertersheuser, S. Mensing, R. Humerickhouse, W. Awni, H. Xiong, Mechanism-based pharmacokinetic/pharmacodynamic meta-analysis of navitoclax (ABT-263) induced thrombocytopenia, Cancer Chemother. Pharmacol. 74 (2014) 593–602, https://doi.org/10.1007/S00280-014-2530-9.
[77] Y. He, X. Zhang, J. Chang, H.N. Kim, P. Zhang, Y. Wang, S. Khan, X. Liu, X. Zhang, D. Lv, L. Song, W. Li, D. Thummuri, Y. Yuan, J.S. Wiegand, Y.T. Ortiz, V. Budamagunta, J.H. Elisseeff, J. Campisi, M. Almeida, G. Zheng, D. Zhou, Using proteolysis-targeting chimera technology to reduce navitoclax platelet toxicity and improve its senolytic activity, Nat. Commun. 11 (2020), https://doi.org/10.1038/s41467-020-15838-0.
[78] A. Agostini, L. Mondragón, A. Bernardos, R. Martínez-Máñez, M. Dolores Marcos, F. Sancenõn, J. Soto, A. Costero, C. Manguan-García, R. Perona, M. Moreno-Torres, R. Aparicio-Sanchis, J.R. Murguía, L. Mondragon, A. Bernardos, R. Martinez-Mañez, M. Dolores Marcos, F. Sancenon, J. Soto, A. Costero, C. Manguan-Garcia, R. Perona, M. Moreno-Torres, R. Aparicio-Sanchis, J.R. Murguia, Targeted cargo delivery in senescent cells using capped mesoporous silica nanoparticles, Angew. Chem. - Int. Ed. 51 (2012) 10556–10560, https://doi.org/10.1002/anie.201204663.
[79] B. Lozano-Torres, J.F. Blandez, I. Galiana, A. García-Fernández, M. Alfonso, M. D. Marcos, M. Orzáez, F. Sancenón, R. Martínez-Máñez, Real-time in vivo detection of cellular senescence through the controlled release of the NIR fluorescent dye Nile Blue, Angew. Chem. - Int. Ed. 59 (2020) 15152–15156, https://doi.org/10.1002/anie.202004142.
[80] A. Guerrero, R. Guiho, N. Herranz, A. Uren, D.J. Withers, J.P. Martínez-Barbera, L. F. Tietze, J. Gil, Galactose-modified duocarmycin prodrugs as senolytics, Aging Cell 19 (2020), https://doi.org/10.1111/ACEL.13133.
[81] Y. Cai, H. Zhou, Y. Zhu, Q. Sun, Y. Ji, A. Xue, Y. Wang, W. Chen, X. Yu, L. Wang, H. Chen, C. Li, T. Luo, H. Deng, Elimination of senescent cells by β-galactosidase-targeted prodrug attenuates inflammation and restores physical function in aged mice, Cell Res. 30 (2020) 574–589, https://doi.org/10.1038/S41422-020-0314-9.